Inorganic Chemistry

ARTICLE

pubs.acs.org/IC

# Hole Tunneling and Hopping in a $Ru(bpy)_3^{2+}$-Phenothiazine Dyad with a Bridge Derived from oligo-*p*-Phenylene

Mathieu E. Walther[†] and Oliver S. Wenger*

Institut für Anorganische Chemie, Georg-August-Universität Göttingen, Tammannstrasse 4, D-37077 Göttingen, Germany

Supporting Information

**ABSTRACT:** A molecular dyad was synthesized in which a $Ru(bpy)_3^{2+}$ (bpy = 2,2′-bipyridine) photosensitizer and a phenothiazine redox partner are bridged by a sequence of tetramethoxybenzene, *p*-dimethoxybenzene, and *p*-xylene units. Hole transfer from the oxidized metal complex to the phenothiazine was triggered using a flash-quench technique and investigated by transient absorption spectroscopy. Optical spectroscopic and electrochemical experiments performed on a suitable reference molecule in addition to the above-mentioned dyad lead to the conclusion that hole transfer from $Ru(bpy)_3^{3+}$ to phenothiazine proceeds through a sequence of hopping and tunneling steps: Initial hole hopping from $Ru(bpy)_3^{3+}$ to the easily oxidizable tetramethoxybenzene unit is followed by tunneling through the barrier imposed by the *p*-dimethoxybenzene and *p*-xylene spacers. The overall charge transfer proceeds with a time constant of 41 ns, which compares favorably to a time constant of 1835 ns associated with equidistant hole tunneling between the same donor−acceptor couple bridged by three identical *p*-xylene units. The combined hopping/tunneling sequence thus leads to an acceleration of hole transfer by roughly a factor of 50 when compared to a pure tunneling mechanism.

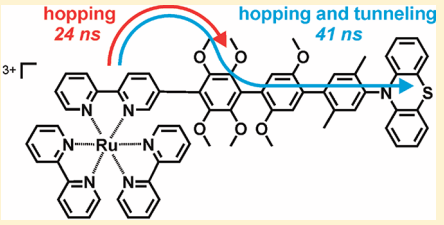


## INTRODUCTION

Long-range charge transfer in donor-bridge-acceptor systems can proceed through tunneling or hopping mechanisms.[1] As long as the one-electron reduced or oxidized states of the bridge cannot be populated directly by the transferring charge carriers, superexchange-mediated tunneling is the only viable reaction mechanism. This is typically the case for alkane bridges,[2] weakly $\pi$-conjugated molecular rods,[3] and for many proteins.[4] As soon as there are easily reducible or oxidizable molecular units in the bridge, electron or hole hopping may become important. This is observed for example in strongly $\pi$-conjugated molecular wires,[5] in DNA,[6] and in proteins in which the charge transfer pathway includes amino acids with redox-active side chains.[7]

Oligo-*p*-phenylene bridges of short length mediate charge transfer via the tunneling mechanism, while longer congeners enable the hopping process.[8] Through substitution of phenylene moieties with electron-donating substituents the oxidation potentials of individual bridging units can be tuned deliberately, and this may be exploited for accelerating hole transfer.[9] For instance, hole transfer across four *p*-dimethoxybenzene units was found to be more than 3 orders of magnitude more rapid than equidistant hole transfer (between the same donor−acceptor couple) across four *p*-xylene spacers.[10]

Here, we report on phototriggered long-range charge transfer in a molecular dyad (Ru−PTZ) in which a $Ru(bpy)_3^{2+}$ photosensitizer and a phenothiazine (PTZ) reaction partner are bridged by a sequence of tetramethoxybenzene (tmb), *p*-dimethoxybenzene (dmb), and *p*-xylene (xy) units (Scheme 1). A reference molecule (Ru−H), containing the exact same molecular components except the phenothiazine moiety, was investigated simultaneously. A dyad composed of the same donor−acceptor couple bridged by three identical *p*-xylene spacers, hereafter referred to as Ru−$xy_3$-PTZ, was available from a prior investigation and served as an additional reference molecule.[11]

## RESULTS AND DISCUSSION

**Synthesis.** Synthesis of the organic molecular rods required for dyad Ru−PTZ and reference molecule Ru−H followed the strategy shown in Scheme 2. Phenothiazine (**1**) was coupled to 1-bromo-4-trimethylsilyl-2,5-dimethylbenzene (**2**)[12] using a palladium(0) catalyst. The trimethylsilyl-protected reaction product (**3**) was converted to iodo-compound **4** with iodine monochloride. Subsequent Suzuki-coupling with 2,5-dimethoxy-4-trimethylsilyl-1-phenylboronic acid (**5**)[10] elongated the molecular bridge by one unit (**6**). Trimethylsilyl/halogen exchange gave product **7**, which was further elongated by reaction with 4-trimethylsilyl-2,3,5,6-tetramethoxyl-1-phenylboronic acid (**8**).[9c] An additional trimethylsilyl/halogen exchange converted the Suzuki coupling product **9** to the activated iodo-compound **10**. The latter was reacted with 5-(tri(*n*-butyltin)-2,2′-bipyridine (**11**)[11] to yield ligand **12**. Reaction with $Ru(bpy)_2Cl_2$[13] then lead to Ru−PTZ. The overall yield from molecule **1** to Ru−PTZ was 0.9%.

Synthesis of the Ru−H reference molecule departed from 1-bromo-2,5-dimethylbenzene (**13**). Each of the two Suzuki-coupling steps (yielding molecules **14** and **16**) with the same boronic acids used already for the dyad (**5**, **8**) was followed by trimethylsilyl/halogen exchange with iodine monochloride (**15**, **17**).

**Received:** July 8, 2011
**Published:** September 29, 2011

**Scheme 1. Chemical Structures of the Molecules Investigated in This Work**[a]

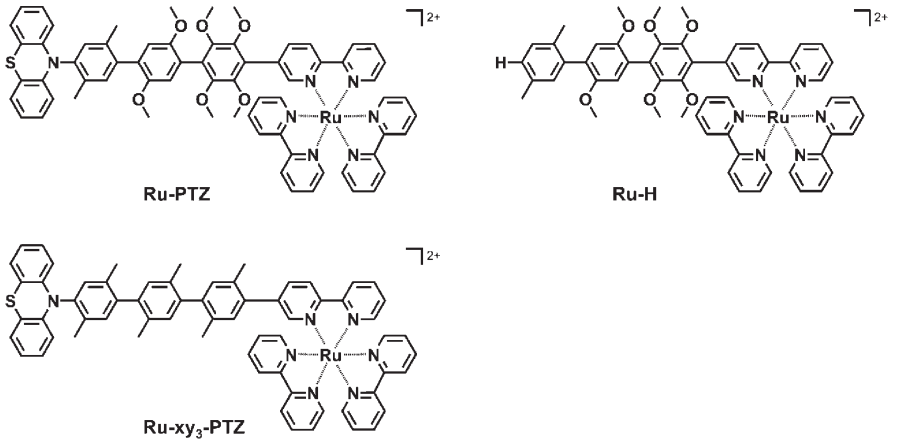


[a] The Ru−$xy_3$-PTZ molecule was available from a prior study and merely used as a reference system.[11a].

**Scheme 2. Synthetic Strategy Leading to the Functionalized Bipyridine Ligands Required for the Ru−PTZ and Ru−H Molecules from Scheme 1**[a]

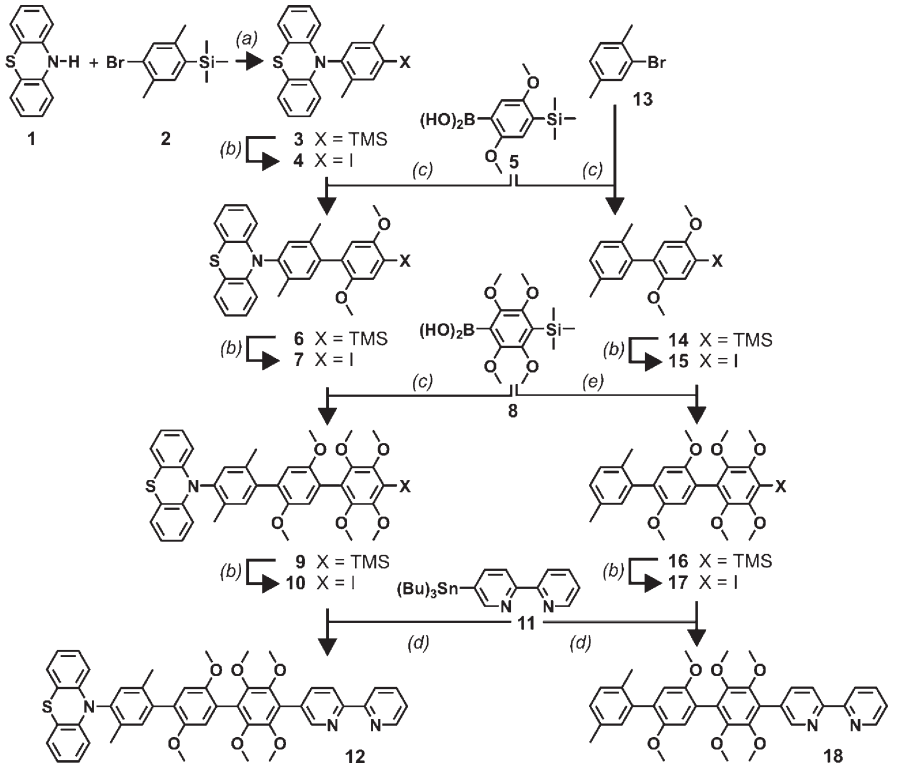


[a] (a) $^t$BuOK, $Pd(dba)_2$, $P(^tBu)_3$, toluene, 80 °C; (b) ICl, $CH_3CN/CH_2Cl_2$ 1:4, 25 °C; (c) $Pd(PPh_3)_4$, $Na_2CO_3$, toluene/water, reflux; (d) $Pd(PPh_3)_4$, *m*-xylene, reflux; (e) $Pd(dba)_2$, $P(^tBu)_3$, $Cs_2CO_3$, dioxane, 60 °C.

Stille-coupling between product **17** and bipyridine **11** gave ligand **18**, which reacted with $Ru(bpy)_2Cl_2$ to reference molecule Ru−H. The overall yield from molecule **12** to Ru−H was 10.8%. Detailed synthetic protocols and characterization data are given in the Supporting Information.

**Optical Absorption and Luminescence.** Figure 1a shows the optical absorption spectra of Ru−PTZ and Ru−H in acetonitrile solution at room temperature along with the electronic spectrum of $Ru(bpy)_3^{2+}$ measured under the same conditions. In all three cases the lowest energetic absorption feature (around 450 nm) is the metal-to-ligand charge transfer (MLCT) band. At 288 nm, there is a prominent band due to a bpy-localized $\pi-\pi^*$ transition, and in Ru−PTZ an analogous phenothiazine-localized transition manifests itself with a peak at 257 nm. Compared to $Ru(bpy)_3^{2+}$, there is additional absorption intensity in Ru−PTZ and Ru−H between 300 and 390 nm. A similar observation was made for ruthenium-phenothiazine dyads with oligo-*p*-dimethoxybenzene bridges,[10] and to lesser extent for oligo-*p*-xylene bridged


dx.doi.org/10.1021/ic201446x |*Inorg. Chem.* 2011, 50, 10901–10907

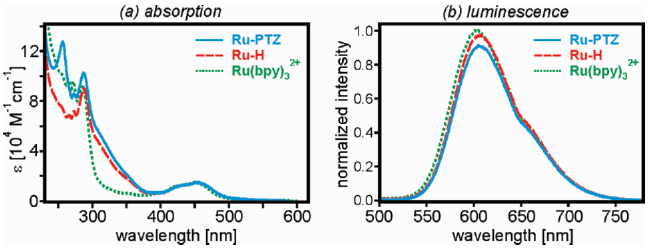


**Figure 1.** (a) Optical absorption spectra of Ru−PTZ, Ru−H, and $Ru(bpy)_3^{2+}$ in acetonitrile at room temperature. (b) Luminescence of these three species under identical conditions. Excitation occurred at 450 nm; the relative intensities are corrected for differences in absorbance at the excitation wavelength and were normalized to a value of 1.0 for the $Ru(bpy)_3^{2+}$ sample.

analogues.[11] Thus, the additional absorption intensity between 300 and 390 nm is likely due to the bridge, with a dominant contribution from the di- and tetramethoxybenzene units.

Figure 1b shows that the emission spectra and intensities of Ru−PTZ, Ru−H, and $Ru(bpy)_3^{2+}$ are nearly identical. Notably, there is no luminescence quenching in the dyad, as would be expected if there was efficient photoinduced electron transfer from the phenothiazine to the photoexcited $Ru(bpy)_3^{2+}$. The same observation was made previously for other $Ru(bpy)_3^{2+}$-PTZ systems, and it is commonly explained by the very low driving force for photoinduced electron transfer between these two reaction partners.[14] Our own electrochemical investigations of Ru−PTZ and Ru−H, discussed below, are consistent with this interpretation. Transient absorption difference spectra of Ru−PTZ and Ru−H in acetonitrile are shown in the Supporting Information, Figure S1. They exhibit the common features associated with the $^3$MLCT excited state of the $Ru(bpy)_3^{2+}$ unit, namely, absorption maxima around 375 and 545 nm due to bpy radical anion, as well as a bleach around 450 nm due to loss of MLCT intensity.[15] As seen from the Supporting Information, Figure S2, the transient absorption signals at these wavelengths decay with essentially the same time constant as the luminescence intensity at 610 nm. Identical $^3$MLCT excited-state lifetimes of 190 ns are derived from these data for Ru−PTZ and Ru−H in aerated acetonitrile solution. For reference, $Ru(bpy)_3^{2+}$ has a lifetime of 170 ns under identical conditions.[16]

**Electrochemistry.** Figure 2 shows cyclic voltammograms measured on deoxygenated acetonitrile solutions of Ru−PTZ (solid blue line in the upper half) and Ru−H (dashed red line in the lower half) in presence of 0.1 M tetrabutylammonium hexafluorophosphate electrolyte. The waves centered at 0.0 V are due to the ferrocenium/ferrocene ($Fc^+$/Fc) couple, which was used as an internal standard and as a reference point for all other redox couples reported in this work. The only significant difference between the two voltammograms in Figure 2 is the occurrence of a (quasi-reversible) wave at 0.30 V vs $Fc^+$/Fc in the Ru−PTZ dyad and the absence of this signal in the voltammogram of Ru−H. Consequently, this wave is assigned to the $PTZ^{\bullet+}$/PTZ couple, in good agreement with previously reported values for $PTZ^{\bullet+}$ reduction potentials.[14,17] Our initial expectation was that a wave associated with the $tmb^{\bullet+}$/tmb redox couple would be observable around 0.42 V vs $Fc^+$/Fc in both Ru−PTZ and Ru−H, based on a previous study which reports a redox potential of 0.80 V vs SCE for the tetramethoxybenzene molecule (Table 1).[18] The experiment shows that neither Ru−PTZ nor Ru−H exhibits any redox wave between 0.0 and 0.8 V vs

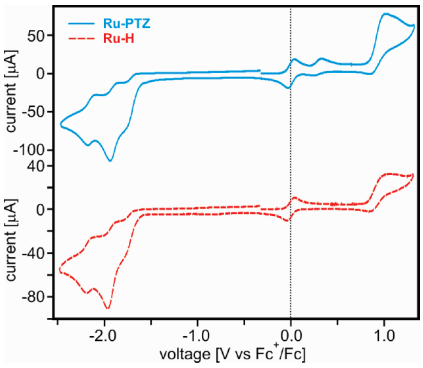


**Figure 2.** Cyclic voltammograms obtained for Ru−PTZ (solid blue line) and Ru−H (dashed red line) in acetonitrile solution with 0.1 M tetrabutylammonium hexafluorophosphate electrolyte. The wave at 0.0 V is due to the ferrocenium/ferrocene couple, which was added to the solution as an internal reference. The scan rate was 100 mV/s.

**Table 1. Electrochemical Potentials for the Individual Redox-Active Components of the Ru−PTZ and Ru−H Molecules, As Observed Either Directly within the Respective Molecular Ensembles or As Individual Units Free in Solution** [a]

| | in molecular ensemble | | |
|---|---|---|---|
| | Ru−PTZ | Ru−H | free in solution |
| $PTZ^{\bullet+/0}$ | 0.30 | N/A | 0.37[b] |
| $tmb^{\bullet+/0}$ | (0.8 < *x* < 1.1) | (0.8 < *x* < 1.1) | 0.42[c] |
| $dmb^{\bullet+/0}$ | 1.10 | | 0.96[c] |
| $xy^{\bullet+/0}$ | | | 1.68[c] |
| Ru(III/II) | 0.93 | 0.93 | 0.89[d] |
| $bpy^{-/0}$ | −1.74 | −1.74 | −1.68[e] |
| $bpy^{-/0}$ | −1.92 | −1.92 | −1.88[e] |
| $bpy^{-/0}$ | −2.18 | −2.18 | −2.15[e] |

[a] All potentials are given in Volts versus $Fc^+$/Fc. Literature values reported in Volts versus SCE were converted to Volts versus $Fc^+$/Fc by subtracting 0.38 V. [b] From ref 14. [c] From ref 18. [d] From ref 20. [e] From ref 19.

$Fc^+$/Fc, and we are forced to conclude that oxidation of tmb incorporated into Ru−PTZ and Ru−H occurs at potentials more positive than 0.8 V vs $Fc^+$/Fc. It is possible that oxidation of the tmb unit in our molecules is more difficult than usual because it is attached directly to the dicationic $Ru(bpy)_3^{2+}$ unit.

The redox wave associated with the Ru(III)/Ru(II) couple is expected around 1.0 V vs $Fc^+$/Fc,[19] and indeed one observes a prominent wave close to this potential for both Ru−PTZ and Ru−H. However, these waves are significantly broader and less reversible than for $Ru(bpy)_3^{2+}$ alone. This may indicate that the Ru(III)/Ru(II) and $tmb^{\bullet+}$/tmb redox waves occur in fact at similar potential. The midpoint between the maxima in the oxidative and reductive sweeps is at 0.93 V vs $Fc^+$/Fc, and this value is taken as the redox potential for the Ru(III)/Ru(II) couple (Table 1).

At 1.10 V vs $Fc^+$/Fc a weak wave is observable in the oxidative sweep of the voltammogram of Ru−PTZ. This wave coincides with that previously observed for dimethoxybenzene bridging units in a chemically similar ruthenium-phenothiazine dyad,[10] and therefore is assigned to the $dmb^{\bullet+}$/dmb redox couple. The $xy^{\bullet+}$/xy


dx.doi.org/10.1021/ic201446x |Inorg. Chem. 2011, 50, 10901–10907

**Scheme 3. Graphical Illustration of the Flash-Quench Technique Used for Phototriggering of Intramolecular Charge Transfer between Ru(III) and PTZ in the Ru−PTZ Dyad**

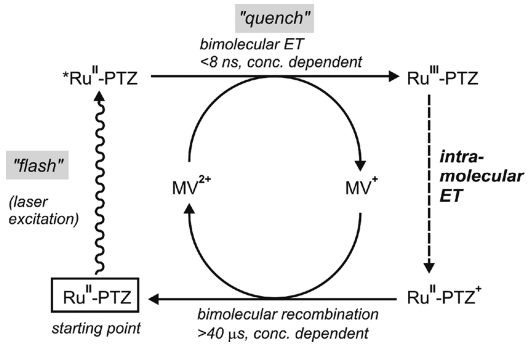


couple would be expected around 1.68 V vs $Fc^+/Fc$,[18] but this is beyond the potential window that could be probed in our experiment.

Table 1 contains a summary of all relevant reduction potentials, including the values for bpy-localized reductions. Given a $^3$MLCT energy of 2.12 eV, one estimates an electrochemical potential of 0.38 V vs $Fc^+/Fc$ for reduction of the photoexcited $Ru(bpy)_3^{2+}$ complex in Ru−PTZ.[20] Thus, electron transfer from PTZ to the excited photosensitizer is exergonic by only 0.08 eV, which explains the lack of significant emission quenching in the dyad when compared to Ru−H or free $Ru(bpy)_3^{2+}$.

**Flash-Quench Technique.** Since the photoexcited $Ru(bpy)_3^{2+}$ complex in Ru−PTZ is not a sufficiently potent electron acceptor, the more oxidizing $Ru(bpy)_3^{3+}$ complex had to be generated photochemically to trigger intramolecular charge transfer. This was possible using a so-called flash-quench technique, as illustrated in Scheme 3. This is a method that has been applied successfully in many prior investigations of long-range charge transfer in proteins,[21] as well as for studies of (proton-coupled) electron transfer in artificial systems.[22] After photoexcitation ("flash"), the $^3$MLCT excited-state of the $Ru(bpy)_3^{2+}$ moiety is quenched oxidatively using excess methylviologen dication ($MV^{2+}$). At sufficiently high methylviologen concentrations (here ∼50 mM) the "quench" step occurs within the duration of a nanosecond laser pulse. Given that the intramolecular charge transfer is sufficiently slow, one may thus observe a maximal amount of Ru(III) and $MV^{\bullet+}$ immediately after the laser pulse. Subsequent intramolecular charge transfer then leads to reduction of Ru(III) to Ru(II) and oxidation of PTZ to $PTZ^{\bullet+}$. The reduced methylviologen reacts with the oxidized dyad only on a 40 $\mu$s-time scale; hence, when using the reversible $MV^{2+}$ quencher, there is usually a time window ranging from ∼8 ns to ∼40 $\mu$s in which intramolecular charge transfer can be monitored.[21] Importantly, the Ru(III), $PTZ^{\bullet+}$, and $MV^{\bullet+}$ photoredox products can all be detected easily and unambiguously by transient absorption spectroscopy.

**Transient Absorption and Spectroelectrochemistry.** Figure 3a shows transient absorption spectra measured on room temperature acetonitrile solutions containing $\sim 10^{-4}$ M Ru−PTZ (solid blue line) or Ru−H (dashed red line) in presence of 50 mM methylviologen dication. Detection occurred in a time window of 200 ns width, starting immediately after the 8-ns laser pulse. The most prominent features in both spectra are those of methylviologen radical

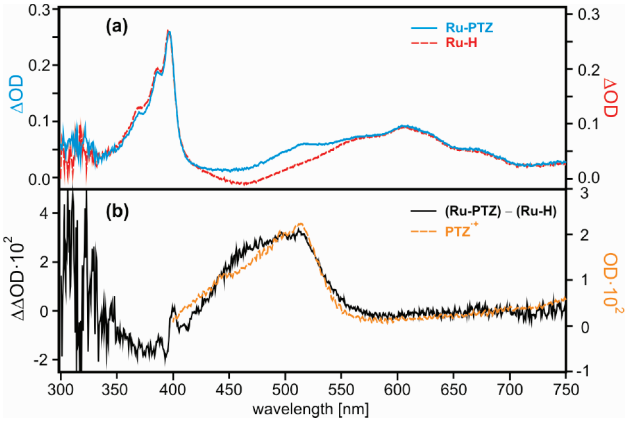


**Figure 3.** (a) Transient absorption spectra measured on $\sim 10^{-4}$ M acetonitrile solutions of Ru−PTZ (solid blue line) and Ru−H (dashed red line) in presence of 50 mM methylviologen. Excitation occurred with 8 ns laser pulses at 450 nm; the signal was detected in a 200 ns time window starting immediately after the laser pulse. (b) The solid black trace is the result of a mathematical subtraction of the transient absorption spectrum of Ru−H from the transient absorption spectrum of Ru−PTZ. The dashed orange line is the absorption spectrum of $PTZ^{\bullet+}$, measured in a spectroelectrochemical experiment using a PTZ reference molecule in dichloromethane solution. The exact chemical structure of this reference molecule is shown in the Supporting Information, Scheme S1.

monocation ($MV^{\bullet+}$), namely, an intense and structured band with an absorption maximum at 397 nm and a less intense, broader band with a maximum at 607 nm. The two spectra in Figure 3a differ from each other only in the spectral region between 420 and 570 nm. When the transient absorption spectrum of Ru−H is subtracted from the spectrum of Ru−PTZ, the solid black line shown in Figure 3b is obtained. Superimposed on this derived spectrum is the absorption spectrum of $PTZ^{\bullet+}$ (dashed orange trace), measured in a spectroelectrochemistry experiment using a suitable reference molecule (the precise chemical structure of which is shown in the Supporting Information, Scheme S1).[23] We conclude from this comparison that the additional intensity between 420 and 570 nm in the transient absorption spectrum of Ru−PTZ is due to $PTZ^{\bullet+}$. The absorption maximum of the $PTZ^{\bullet+}$ species in this case is at 517 nm.

Figure 4 shows the temporal evolution of some relevant transient absorption signals of Ru−PTZ (blue traces on the left) and Ru−H (red traces on the right) in the first 300 ns after the laser excitation pulse. The transient absorption signal of Ru−PTZ at 397 nm (top panel), identified above as due to $MV^{\bullet+}$, rises with a time constant of 8 ns, which corresponds to the time resolution of the equipment used for these experiments. Logically, the rise of the signal at 607 nm (bottom panel) is equally fast, because it is caused by the same species ($MV^{\bullet+}$). By contrast, at 517 nm where $PTZ^{\bullet+}$ has its absorption maximum (middle panel), an initial fast rise (solid line) is followed by a significantly slower increase in intensity (dashed line). The initial fast rise occurs with a time constant of 8 ns, and is attributed to the rapid formation of $MV^{\bullet+}$, while the slower rise occurs with a time constant of 41 ns.

From Figure 3a it can be seen that the overall absorption intensity at 517 nm in Ru−PTZ is caused by $MV^{\bullet+}$ and $PTZ^{\bullet+}$ to roughly equal extent, which explains the biexponential shape of the rise shown in the middle panel of Figure 4a. In the Ru−H


dx.doi.org/10.1021/ic201446x |Inorg. Chem. 2011, 50, 10901–10907

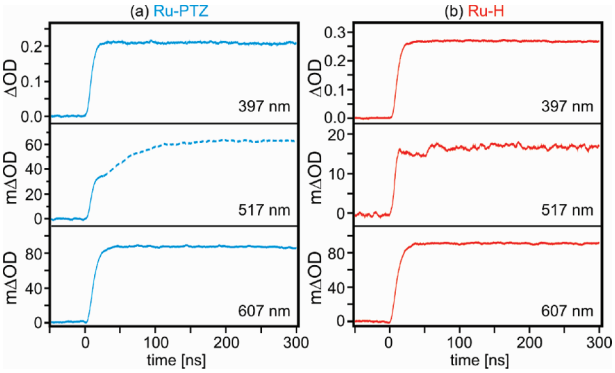


**Figure 4.** Temporal evolution of the transient absorption signals from Figure 3a at selected detection wavelengths for Ru−PTZ (left) and Ru−H (right).

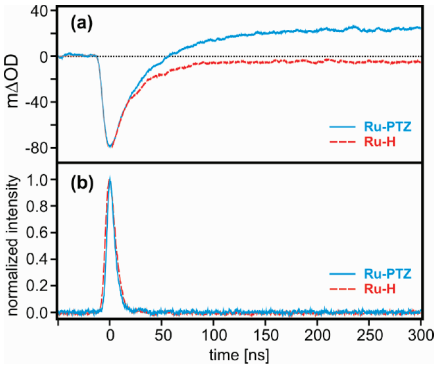


**Figure 5.** (a) Temporal evolution of the transient absorption signal at 465 nm in Ru−PTZ (solid blue trace) and Ru−H (dashed red trace) in the first 300 ns after initiation of the flash-quench sequence. (b) Temporal evolution of the luminescence intensity at 610 nm in the same samples, i.e., in presence of 50 mM methylviologen.

reference system, detection at 517 nm yields a transient of significantly weaker intensity and a rise nearly identical to those observable at 397 and 607 nm. These observations are consistent with our interpretations, and we may conclude that in the Ru−PTZ dyad, $PTZ^{\bullet+}$ formation occurs with a time constant of 41 ns after photogeneration of Ru(III).

$PTZ^{\bullet+}$ formation may be regarded as "electron departure" from the phenothiazine unit, and if an intramolecular charge transfer process is active in our Ru−PTZ dyad, it should be possible to observe "electron arrival" at the Ru(III) center. Indeed, this is possible by monitoring the transient absorption signal at 465 nm, where $Ru(bpy)_3^{3+}$ absorbs weakly compared to $Ru(bpy)_3^{2+}$, that is, at the so-called MLCT bleach. The transient obtained for Ru−PTZ at this wavelength is shown in Figure 5a (solid blue line).

Recovery of the bleach occurs in a biexponential fashion, with time constants of 24 and 41 ns. The latter is again due to the $PTZ^{\bullet+}$ species, which absorbs weakly at the detection wavelength of 465 nm (Figure 3b). In Figure 5a this shows up very clearly in a rise of the transient absorption signal to positive ΔOD values at times longer than 55 ns. Importantly, the faster time constant of 24 ns does not only show up in the biexponential bleach recovery of Ru−PTZ (solid blue line); it is also observed in the single exponential MLCT bleach recovery of the Ru−H reference molecule

**Scheme 4. Illustration of the Intramolecular Hole Transfer Process and Its Energetics in the Ru−PTZ Dyad[a]**

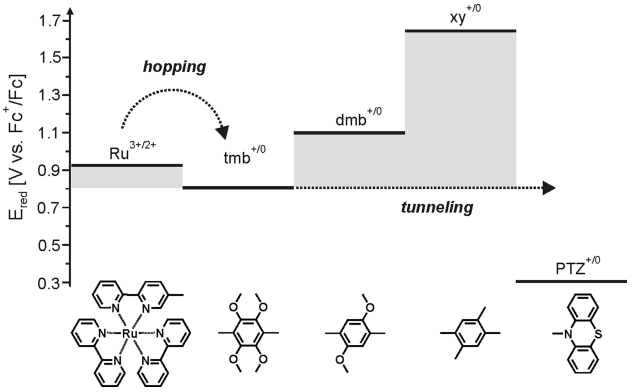


[a] The solid horizontal lines represent redox potentials of the individual molecular components.

(dashed red line). The inescapable conclusion from this is that Ru(III) reduction occurs independently of PTZ oxidation. Although we have been unable to determine the precise value of the tetramethoxybenzene (tmb) redox potential (see above), Table 1 indicates that the tmb unit is the only redox-active component in Ru−PTZ and Ru−H with sufficient reducing power for conversion of Ru(III) to Ru(II). Thus, it appears plausible to conclude that once Ru(III) has been formed, it is reduced by tmb to Ru(II), and $tmb^{\bullet+}$ is formed at the same time. We have been unable to detect the $tmb^{\bullet+}$ radical cation even in Ru−H, presumably because its signal is hidden by more intense transient absorption signals from $MV^{\bullet+}$.[24] At any rate, the luminescence decay traces in Figure 5b (detected at 610 nm) show that the formation of Ru(III) is complete within 8 ns in both Ru−PTZ and Ru−H, and consequently the time constant of 24 ns determined for Ru(III) disappearance is genuine.

**Hole Hopping and Tunneling.** The previous section has led us to the conclusion that "electron departure" at the PTZ site occurs with a time constant of 41 ns, while "electron arrival" at the ruthenium(III) complex is associated with a time constant of only 24 ns. This can be understood in the framework of an overall charge transfer process which is composed of a sequence of hopping and tunneling steps, as illustrated in Scheme 4. This Scheme shows the electrochemical potentials for one-electron oxidation of the individual molecular components of the Ru−PTZ dyad as horizontal lines, that is, we use a hole transfer picture for discussion of the overall charge transfer event. This is meaningful because the one-electron oxidized states of the bridging tmb, dmb, and xy units are energetically much closer to the relevant donor and acceptor states than the one-electron reduced bridge states.[18] The flash-quench procedure forms a highly energetic hole at the ruthenium site within 8 ns. From there, the hole is transferred to tmb within 24 ns, which may be considered a hopping step between nearest neighbors. Given the short distance between $Ru(bpy)_3^{3+}$ and tmb, this process is relatively slow. The likely reason for this is its low driving force. One may use the transient absorption data in Figure 5a to estimate the driving force for hole hopping from $Ru(bpy)_3^{3+}$ to tmb:[25] The Ru−H reference molecule (red trace) exhibits a persistent, barely noticeable bleach (with an average ΔOD-value of −0.005) at times longer than 100 ns which can be attributed to Ru(III) in metastable equilibrium with $tmb^{\bullet+}$. The initial ΔOD-value at the


dx.doi.org/10.1021/ic201446x |Inorg. Chem. 2011, 50, 10901–10907

time of laser excitation amounts to −0.815, which leads us to an equilibrium constant of 163 in favor of $tmb^{\bullet+}$ formation, and thus Ru(III) to tmb hole hopping is estimated to be exergonic by 0.13 eV.

By contrast, hole transfer from the initial Ru(III) state to dmb is endergonic by at least 0.17 eV; hence, for the second bridging unit, hopping becomes more difficult, and for the xy unit it can be ruled out completely because of the very high oxidation potential of this particular spacer.[18] The most plausible mechanistic scenario for the overall charge transfer process in Ru−PTZ is captured by the two dashed arrows in Scheme 4: After an initial hole transfer from Ru(III) to tmb via hopping between nearest neighbors, the hole tunnels through the barrier imposed by the dmb and xy bridging units. This picture is consistent will all experimental data.

## SUMMARY AND CONCLUSIONS

A combination of hopping and tunneling steps is responsible for phototriggered hole transfer in the Ru−PTZ dyad. The Ru−$xy_3$-PTZ dyad from Scheme 1 is a suitable reference point to illustrate the efficiency of the overall Ru(III)-to-PTZ hole transfer process in the Ru−PTZ molecule: In both dyads charge transfer occurs between identical redox couples over the same distance, but in Ru−$xy_3$-PTZ a pure tunneling mechanism is operative. The time constants for hole transfer in the two systems are 41 and 1835 ns, that is, the hopping/tunneling sequence in Ru−PTZ is almost a factor of 50 more rapid than the tunneling process in Ru−$xy_3$-PTZ.

In a prior study of variable-length Ru−$xy_n$-PTZ molecules ($n = 1 - 4$) we determined a distance decay constant of 0.77 $Å^{-1}$ for hole tunneling from photogenerated $Ru(bpy)_3^{3+}$ to phenothiazine across oligo-*p*-xylene bridges.[11a] The length of a single *p*-xylene unit is 4.3 Å, and consequently the hole transfer rate increases by a factor of 27 per unit omitted. The factor-of-50 rate acceleration found above for the Ru−PTZ system is therefore predominantly the result of a shorter tunneling distance. Contrary to prior studies by us and others,[3c,9,10,27] the (local) lowering of the barrier for hole tunneling caused by the *p*-dimethoxybenzene unit appears to play a comparatively small role in this particular instance.

Our present study provides an illustrative example for how alteration of bridge redox potentials through attachment of chemical substituents can affect the rates for charge transfer between distant donors and acceptors. Tetramethoxybenzene units appear to be promising hopping stations in oligo-*p*-phenylene bridges.

## EXPERIMENTAL SECTION

Commercially available chemicals were used as received without further purification. Where needed, solvents were dried using standard methods. Detailed synthetic protocols and characterization data for Ru−PTZ and Ru−H, as well as for all intermediates from Scheme 2 are given in the Supporting Information. $^1$H NMR spectra were acquired on a Bruker Avance 400 MHz spectrometer; electrospray mass spectrometry was performed on Finnigan MAT SSQ 7000 and QSTAR XL (AB/MDS Sciex) instruments. Elemental analyses were conducted by Dr. Hansjörg Eder from the School of Pharmaceutical Sciences at the University of Geneva. Optical absorption spectroscopy was performed using a Cary 300 spectrophotometer from Varian, and steady-state luminescence spectra were measured on a Fluorolog-3 instrument from Horiba Jobin-Yvon. For transient absorption spectroscopy and time-resolved emission experiments, an LP920-KS instrument from Edinburgh Instruments, equipped with an iCCCD camera from Andor, was used. The excitation source was a Quantel Brilliant b laser equipped with an OPO from Opotek. A Versatat3-100 potentiostat from Princeton Applied Research was used for cyclic voltammetry and spectroelectrochemistry. For cyclic voltammetry, a glassy carbon working electrode was employed, and two silver wires served as a counter-electrode and quasi-reference electrode. Spectroelectrochemical measurements were performed using an OTTLE cell (Omni-cell from Specac).[26]

## ASSOCIATED CONTENT

**Supporting Information.** Detailed synthetic protocols and characterization data, additional spectroscopic data. This material is available free of charge via the Internet at http://pubs.acs.org.

## AUTHOR INFORMATION

### Corresponding Author

*Phone: +49 (0)551 39 19424. Fax: +49 (0)551 3373. E-mail: oliver.wenger@chemie.uni-goettingen.de.

### Present Address

†Arizona State University, Department of Chemistry and Biochemistry, Tempe, AZ 85287-1604.

## ACKNOWLEDGMENT

Financial support from the Deutsche Forschungsgemeinschaft through Grants WE4815/1 and INST186/872-1 is gratefully acknowledged. We thank Bice He for cyclic voltammetry measurements.

## REFERENCES

(1) (a) Gray, H. B.; Winkler, J. R. *Proc. Natl. Acad. Sci. U. S. A.* **2005**, *102*, 3534–3539. (b) Cordes, M.; Giese, B. *Chem. Soc. Rev.* **2009**, *38*, 892–901.

(2) (a) Calcaterra, L. T.; Closs, G. L.; Miller, J. R. *J. Am. Chem. Soc.* **1983**, *105*, 670–671. (b) Oevering, H.; Paddon-Row, M. N.; Heppener, M.; Oliver, A. M.; Cotsaris, E.; Verhoeven, J. W.; Hush, N. S. *J. Am. Chem. Soc.* **1987**, *109*, 3258–3269. (c) Wenger, O. S.; Leigh, B. S.; Villahermosa, R. M.; Gray, H. B.; Winkler, J. R. *Science* **2005**, *307*, 99–102.

(3) (a) Indelli, M. T.; Chiorboli, C.; Flamigni, L.; De Cola, L.; Scandola, F. *Inorg. Chem.* **2007**, *46*, 5630–5641. (b) Rosokha, S. V.; Sun, D.-L.; Kochi, J. K. *J. Phys. Chem. A* **2002**, *106*, 2283–2292. (c) Wenger, O. S. *Acc. Chem. Res.* **2011**, *44*, 25–35.

(4) (a) Gray, H. B.; Winkler, J. R. *Annu. Rev. Biochem.* **1996**, *65*, 537–561. (b) Schanze, K. S.; Cabana, L. A. *J. Phys. Chem.* **1990**, *94*, 2740–2743. (c) Marshall, J. L.; Stobart, S. R.; Gray, H. B. *J. Am. Chem. Soc.* **1984**, *106*, 3027–3029.

(5) (a) Davis, W. B.; Svec, W. A.; Ratner, M. A.; Wasielewski, M. R. *Nature* **1998**, *396*, 60–63. (b) Sikes, H. D.; Smalley, J. F.; Dudek, S. P.; Cook, A. R.; Newton, M. D.; Chidsey, C. E. D.; Feldberg, S. W. *Science* **2001**, *291*, 1519–1523. (c) Lloveras, V.; Vidal-Gancedo, J.; Figueira-Duarte, T. M.; Nierengarten, J. F.; Novoa, J. J.; Mota, F.; Ventosa, N.; Rovira, C.; Veciana, J. *J. Am. Chem. Soc.* **2011**, *133*, 5818–5833. (d) Giacalone, F.; Segura, J. L.; Martín, N.; Guldi, D. M. *J. Am. Chem. Soc.* **2004**, *126*, 5340–5341. (e) Leatherman, G.; Durantini, E. N.; Gust, D.; Moore, T. A.; Moore, A. L.; Stone, S.; Zhou, Z.; Rez, P.; Liu, Y. Z.; Lindsay, S. M. *J. Phys. Chem. B* **1999**, *103*, 4006–4010. (f) Visoly-Fisher, I.; Daie, K.; Terazono, Y.; Herrero, C.; Fungo, F.; Otero, L.; Durantini, E.; Silber, J. J.; Sereno, L.; Gust, D.; Moore, T. A.; Moore, A. L.; Lindsay, S. M. *Proc. Natl. Acad. Sci. U. S. A.* **2006**, *103*, 8686–8690. (g) Vail, S. A.; Krawczuk, P. J.; Guldi, D. M.; Palkar, A.; Echegoyen, L.; Tome, J. P. C.; Fazio, M. A.; Schuster, D. I. *Chem.—Eur. J.* **2005**, *11*, 3375–3388.

(h) Eng, M. P.; Mårtensson, J.; Albinsson, B. *Chem.—Eur. J.* **2008**, *14*, 2819–2826. (i) Eng, M. P.; Albinsson, B. *Angew. Chem., Int. Ed.* **2006**, *45*, 5626–5629.

(6) (a) Giese, B. *Annu. Rev. Biochem.* **2002**, *71*, 51–70. (b) Genereux, J. C.; Barton, J. K. *Chem. Rev.* **2010**, *110*, 1642–1662. (c) Lewis, F. D.; Letsinger, R. L.; Wasielewski, M. R. *Acc. Chem. Res.* **2001**, *34*, 159–170.

(7) (a) Shih, C.; Museth, A. K.; Abrahamsson, M.; Blanco-Rodriguez, A. M.; Di Bilio, A. J.; Sudhamsu, J.; Crane, B. R.; Ronayne, K. L.; Towrie, M.; Vlček, A.; Richards, J. H.; Winkler, J. R.; Gray, H. B. *Science* **2008**, *320*, 1760–1762. (b) Blanco-Rodríguez, A. M.; Towrie, M.; Sykora, J.; Záliš, S.; Vlček, A. *Inorg. Chem.* **2011**, *50*, 6122–6134. (c) Cordes, M.; Kottgen, A.; Jasper, C.; Jacques, O.; Boudebous, H.; Giese, B. *Angew. Chem., Int. Ed.* **2008**, *47*, 3461–3463. (d) Shafaat, H. S.; Leigh, B. S.; Tauber, M. J.; Kim, J. E. *J. Am. Chem. Soc.* **2010**, *132*, 9030–9039.

(8) (a) Weiss, E. A.; Ahrens, M. J.; Sinks, L. E.; Gusev, A. V.; Ratner, M. A.; Wasielewski, M. R. *J. Am. Chem. Soc.* **2004**, *126*, 5577–5584. (b) Weiss, E. A.; Tauber, M. J.; Kelley, R. F.; Ahrens, M. J.; Ratner, M. A.; Wasielewski, M. R. *J. Am. Chem. Soc.* **2005**, *127*, 11842–11850. (c) Wenger, O. S. *Chem. Soc. Rev.* **2011**, *40*, 3538–3550.

(9) (a) Miller, S. E.; Lukas, A. S.; Marsh, E.; Bushard, P.; Wasielewski, M. R. *J. Am. Chem. Soc.* **2000**, *122*, 7802–7810. (b) Hanss, D.; Walther, M. E.; Wenger, O. S. *Coord. Chem. Rev.* **2010**, *254*, 2584–2592. (c) Hanss, D.; Walther, M. E.; Wenger, O. S. *Chem. Commun.* **2010**, *46*, 7034–7036. (d) Hankache, J.; Wenger, O. S. *Chem. Rev.* **2011**, *111*, 5138–5178.

(10) Walther, M. E.; Wenger, O. S. *ChemPhysChem* **2009**, *10*, 1203–1206.

(11) (a) Hanss, D.; Wenger, O. S. *Inorg. Chem.* **2009**, *48*, 671–680. (b) Hankache, J.; Wenger, O. S. *Chem. Commun.* **2011**, *47*, 10145–10147. (c) Walther, M. E.; Wenger, O. S. *Dalton Trans.* **2008**, 6311–6318.

(12) Hanss, D.; Wenger, O. S. *Inorg. Chem.* **2008**, *47*, 9081–9084.

(13) Sullivan, B. P.; Salmon, D. J.; Meyer, T. J. *Inorg. Chem.* **1978**, *17*, 3334–3341.

(14) (a) Borgström, M.; Johansson, O.; Lomoth, R.; Baudin, H. B.; Wallin, S.; Sun, L. C.; Åkermark, B.; Hammarström, L. *Inorg. Chem.* **2003**, *42*, 5173–5184. (b) Hanss, D.; Wenger, O. S. *Eur. J. Inorg. Chem.* **2009**, 3778–3790.

(15) (a) Milder, S. J.; Gold, J. S.; Kliger, D. S. *J. Phys. Chem.* **1986**, *90*, 548–550. (b) Damrauer, N. H.; Cerullo, G.; Yeh, A.; Boussie, T. R.; Shank, C. V.; McCusker, J. K. *Science* **1997**, *275*, 54–57. (c) Wallin, S.; Davidsson, J.; Modin, J.; Hammarström, L. *J. Phys. Chem. A* **2005**, *109*, 4697–4704.

(16) de Buyl, F.; Kirsch-De Mesmaeker, A.; Tossi, A.; Kelly, J. M. *J. Photochem. Photobiol. A* **1991**, *60*, 27–45.

(17) (a) Chen, P. Y.; Westmoreland, T. D.; Danielson, E.; Schanze, K. S.; Anthon, D.; Neveux, P. E.; Meyer, T. J. *Inorg. Chem.* **1987**, *26*, 1116–1126. (b) Treadway, J. A.; Chen, P. Y.; Rutherford, T. J.; Keene, F. R.; Meyer, T. J. *J. Phys. Chem. A* **1997**, *101*, 6824–6826.

(18) Nicolet, O.; Vauthey, E. *J. Phys. Chem. A* **2002**, *106*, 5553–5562.

(19) (a) Furue, M.; Maruyama, K.; Oguni, T.; Naiki, M.; Kamachi, M. *Inorg. Chem.* **1992**, *31*, 3792–3795. (b) Anderson, P. A.; Keene, F. R.; Meyer, T. J.; Moss, J. A.; Strouse, G. F.; Treadway, J. A. *J. Chem. Soc., Dalton Trans.* **2002**, 3820–3831.

(20) Roundhill, D. M. *Photochemistry and Photophysics of Metal Complexes*; Plenum Press: New York, 1994.

(21) (a) Bjerrum, M. J.; Casimiro, D. R.; Chang, I.-J.; Di Bilio, A. J.; Gray, H. B.; Hill, M. G.; Langen, R.; Mines, G. A.; Skov, L. K.; Winkler, J. R.; Wuttke, D. S. *J. Bioenerg. Biomembr.* **1995**, *27*, 295–302. (b) Mines, G. A.; Bjerrum, M. J.; Hill, M. G.; Casimiro, D. R.; Chang, I. J.; Winkler, J. R.; Gray, H. B. *J. Am. Chem. Soc.* **1996**, *118*, 1961–1965.

(22) (a) Magnuson, A.; Berglund, H.; Korall, P.; Hammarström, L.; Åkermark, B.; Styring, S.; Sun, L. C. *J. Am. Chem. Soc.* **1997**, *119*, 10720–10725. (b) Sjödin, M.; Ghanem, R.; Polivka, T.; Pan, J.; Styring, S.; Sun, L. C.; Sundström, V.; Hammarström, L. *Phys. Chem. Chem. Phys.* **2004**, *6*, 4851–4858. (c) Sjödin, M.; Styring, S.; Wolpher, H.; Xu, Y. H.; Sun, L. C.; Hammarström, L. *J. Am. Chem. Soc.* **2005**, *127*, 3855–3863. (d) Lachaud, T.; Quaranta, A.; Pellegrin, Y.; Dorlet, P.; Charlot, M. F.; Un, S.; Leibl, W.; Aukauloo, A. *Angew. Chem., Int. Ed.* **2005**, *44*, 1536–1540. (e) Hanss, D.; Freys, J. C.; Bernardinelli, G.; Wenger, O. S. *Eur. J. Inorg. Chem.* **2009**, 4850–4859. (f) Wenger, O. S. *Inorg. Chim. Acta* **2011**, *374*, 3–9.

(23) Walther, M. E.; Grilj, J.; Hanss, D.; Vauthey, E.; Wenger, O. S. *Eur. J. Inorg. Chem.* **2010**, 4843–4850.

(24) We were also unable to measure the spectrum of the $tmb^{\bullet+}$ species in a spectroelectrochemical experiment on Ru−H because the $Ru(bpy)_3^{2+}$ complex is oxidized at a similar potential as tmb.

(25) An anonymous reviewer is acknowledged for pointing out this possibility.

(26) Krejčik, M.; Daněk, M.; Hartl, F. *J. Electroanal. Chem.* **1991**, *317*, 179–187.

(27) Lambert, C.; Nöll, G.; Schelter, J. *Nat. Mater.* **2002**, *1*, 69–73.